ACS Infectious Diseases

pubs.acs.org/journal/aidcbc
Article

Enhancing the Intrinsic Antiplasmodial Activity and Improving the Stability and Selectivity of a Tunable Peptide Scaffold Derived from Human Platelet Factor 4

Nicole Lawrence,* Thomas N. G. Handley, Simon J. de Veer, Maxim D. Harding, Alicja Andraszek, Lachlan Hall, Karoline D. Raven, Sandra Duffy, Vicky M. Avery, David J. Craik, Lara R. Malins, and Brendan J. McMorran*

Cite This: *ACS Infect. Dis.* 2024, 10, 2899−2912

Read Online

ACCESS | Metrics & More | Article Recommendations | Supporting Information

ABSTRACT: The control of malaria, a disease caused by *Plasmodium* parasites that kills over half a million people every year, is threatened by the continual emergence and spread of drug resistance. Therefore, new molecules with different mechanisms of action are needed in the antimalarial drug development pipeline. Peptides developed from host defense molecules are gaining traction as anti-infectives due to theood of inducing drug resistance. Human platelet factor 4 (PF4) has intrinsic activity against *P. falciparum*, and a macrocyclic helix−loop−helix peptide derived from its active domain recapitulates this activity. In this study, we used a stepwise approach to optimize first-generation PF4-derived internalization peptides (PDIPs) by producing analogues with substitutions to charged and hydrophobic amino acid residues or with modifications to terminal residues including backbone cyclization. We evaluated the *in vitro* activity of PDIP analogues against *P. falciparum* compared to their overall helical structure, resistance to breakdown by serum proteases, selective binding to negatively charged membranes, and hemolytic activity. Next, we combined antiplasmodial potency-enhancing substitutions that retained favorable membrane and cell-selective properties onto the most stable scaffold to produce a backbone cyclic PDIP analogue with four-fold improved activity against *P. falciparum* compared to first-generation peptides. These studies demonstrate the ability to modify PDIP to select for and combine desirable properties and further validate the suitability of this unique peptide scaffold for developing a new molecule class that is distinct from existing antimalarial drugs.

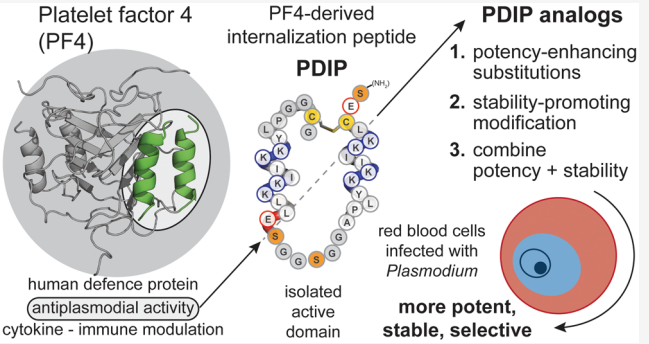

KEYWORDS: *malaria, Plasmodium, host defense peptide, targeted cell-penetration, rational design, drug development*

Malaria is a serious global health burden, killing over 500,000 people every year. Efforts to control the disease saw a decline in the number of deaths between 2000 and 2019, but recent data suggest that the downward trend has stalled, with 608,000 deaths reported in 2022.[1] Factors contributing to this change include the emergence and spread of drug resistance in *Plasmodium falciparum* parasites, insecticide resistance in mosquito vectors that spread the disease, environmental and economic factors, and disruptions to health services due to the COVID-19 pandemic.[2] Artemisinin combination therapies (ACT) have been instrumental in controlling the disease burden since their adoption as the first-line treatment in the early 2000s,[2,3] but this control is under threat with ACT treatment failure reported in South-East Asia and the Western Pacific (incidence summarized by region in the World Malaria report 2023).[1] Artemisinin-resistant *P. falciparum* has also been reported in Africa,[1,4,5] which is especially concerning as this region accounts for 94% of malaria cases globally.[1]

Field surveillance measures that identify resistance to artemisinin derivatives and partner drugs to inform the adoption of different drug combinations are critical in the ongoing battle against drug resistance.[6−8] Rotational use of drug components in combination therapies is a promising strategy for managing resistance,[3,9] and antimalarial drug partners with different mechanisms of action and resistance profiles may serve to prolong the efficacy of individual drug components and circumvent combination therapy failure.[3,9] Even drugs with modest antimalarial efficacy (e.g., antibacterial drugs)[10,11] can be considered if they are refractory to resistance development by

Received: April 9, 2024
Revised: June 12, 2024
Accepted: July 23, 2024
Published: August 1, 2024

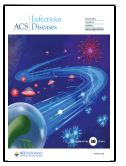

https://doi.org/10.1021/acsinfecdis.4c00276
ACS Infect. Dis. 2024, 10, 2899−2912

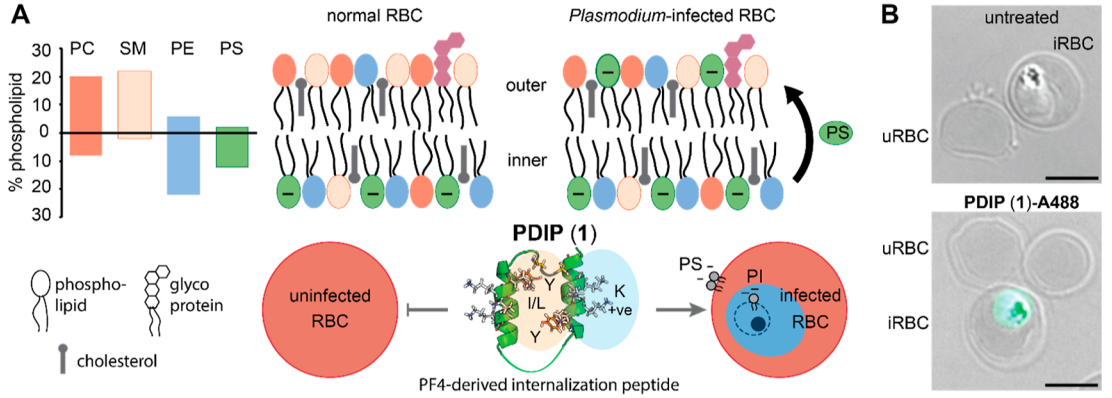

Figure 1. First-generation PF4-derived internalization peptide (PDIP) analogue (cPF4PD, **1**) targets and selectively enters RBCs infected with *P. falciparum*. (A) Normal uninfected RBCs (uRBC) have an asymmetric distribution of lipids, maintaining negatively charged phosphatidylserine (PS) headgroups on the inner leaflet of the cell plasma membrane, whereas PS is also present on the outer leaflet of infected RBCs (iRBC). Percentage RBC phospholipid data from ref 32. PC, phosphatidylcholine; SM, sphingomyelin; PE, phosphatidylethanolamine. (B) PDIP analogue (**1**) labeled with AlexaFluor-488 (A488) has rapid (<1 h) selective entry into iRBC and accumulates inside the parasite. Scale bars are 5 μm.

P. falciparum.[3] Drug discovery efforts have delivered several new small molecule drugs through to validation in clinical trials or *in vivo* studies (reviewed in ref 2). However, *Plasmodium* parasites can rapidly acquire resistance to small-molecule drugs. For example, a single amino acid mutation (G358S) in the target *P. falciparum* ATP4 sodium pump produced clinically relevant resistance to cipargamin, a promising new antimalarial drug candidate.[12,13] To address this rapid rate of acquired resistance, expansion of the discovery efforts to include other classes of bioactive molecules is urgently needed.

Host defense peptides (HDPs), often referred to as antimicrobial peptides (AMPs), are produced by a wide range of organisms.[14,15] HDPs are promising candidates for developing targeted therapies due to their several advantageous properties. They exhibit membrane selectivity that allows distinction between the negatively charged outer membrane leaflets of bacteria,[16] cancer cells,[17,18] and red blood cells (RBCs) infected with *P. falciparum*,[19,20] compared to the neutral surface of healthy mammalian cells. Rather than the discrete single-molecule targets typified by most current drugs, the inherently larger size and interacting surfaces of peptides provide improved target cell selectivity[21] and reduce the likelihood of inducing drug resistance.[22,23] In addition to these properties, some HDPs can cross cell membranes to access intracellular targets.[24−26]

The host defense protein platelet factor 4 (PF4) has intrinsic activity against blood stage *P. falciparum*[27] that can be attributed to short (14 amino acid) AMP-like regions at the C-terminus of each of four subunits.[28,29] Inspired by the paired head-to-tail presentation of these regions in PF4, we engineered a macrocyclic helix−loop−helix peptide (cPF4PD), joined at one end by a flexible linker, and a disulfide bond between introduced Cys residues proximal to the N- and C-termini at the other.[30] cPF4PD kills *P. falciparum in vitro* with similar low micromolar potency to PF4. The mechanism of action involves selective binding to and lysis of membranes that are rich in negatively charged phospholipid headgroups.[30] This selectivity drives entry into infected RBCs, which have increased surface presentation of negatively charged phosphatidylserine (PS) relative to uninfected cells,[19,20] and disruption of the parasite digestive vacuole membrane (Figure 1A), which contains negatively charged phosphatidylinositol 3-phosphate.[31] Notably, cPF4PD does not enter or damage uninfected RBCs at concentrations that inhibit *P. falciparum* growth[30] (Figure 1B).

In this study, we aimed to improve the antiplasmodial potency of the first-generation cPF4PD peptide while maintaining or improving beneficial features including a stable structure that resists proteolysis, and selectivity for infected compared to uninfected RBCs. To achieve these aims, we designed and chemically synthesized two sets of peptide analogues, herein called PF4-derived internalization peptides (PDIPs), to separately identify antiplasmodial potency-enhancing substitutions and scaffold modifications that favor peptide stability. In line with the need for low-cost production of new malaria medicines,[2] we maintained proteinogenic amino acids in the sequence to allow future transfer to biosynthetic production. We assessed each PDIP analogue according to antiplasmodial potency—*in vitro* activity against *P. falciparum*; activity-hemolysis index—antiplasmodial activity relative to lysis of uninfected RBCs; membrane selectivity—binding affinity for negatively charged compared to neutral phospholipid membranes; structure—helicity in aqueous solution; and stability—percentage of recovered intact peptide following incubation with human serum. We combined the best potency-enhancing substitutions with the most stable and selective scaffold to produce a backbone cyclic PDIP analogue with four-fold enhanced *in vitro* activity against *P. falciparum* and a wider window between antiplasmodial activity and hemolysis of uninfected RBCs compared to first-generation analogues. These improvements are an important step toward developing peptide-based drugs to expand the repertoire of drug classes in the antimalarial drug development pipeline.

RESULTS

Two sets of PDIP analogues were designed, with substitutions to charged and hydrophobic residues (set 1) and modification of the C-terminus, including backbone cyclization (set 2). The best potency-enhancing substitutions identified from set 1 were then incorporated onto the most stable scaffold from set 2 to produce analogues with combined optimal modifications. Peptides were produced using Fmoc solid phase synthesis, employing intramolecular native chemical ligation[33,34] for backbone cyclic peptides. Amino acid sequences for the base scaffolds (**1**−**3**), together with cartoon representations of the structure of the parent and modified peptides, are shown in Figure 2. Sequences

https://doi.org/10.1021/acsinfecdis.4c00276
ACS Infect. Dis. 2024, 10, 2899−2912

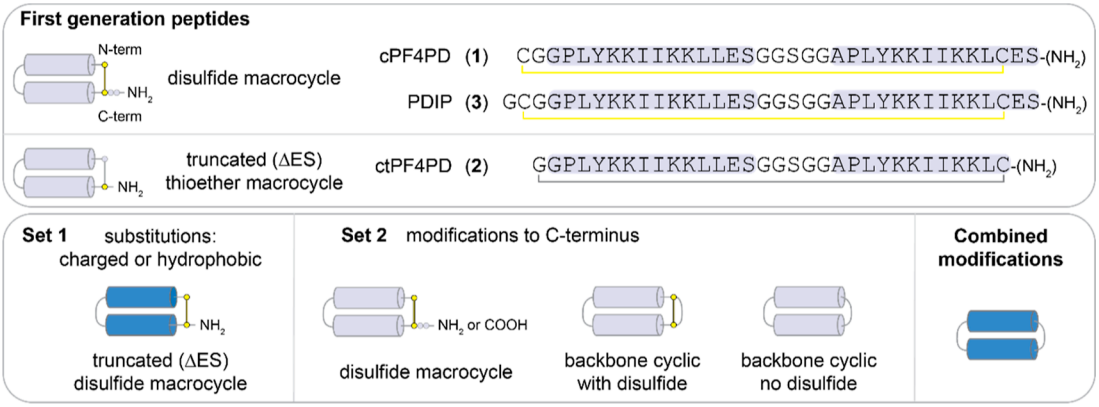

Figure 2. Cartoon Representation of the Structures of PDIP Parent Peptides and Analogues.

Table 1. *In Vitro* Antiplasmodial Activity and Characteristics of PDIP Analogues

Set ID	Peptide	AA change [a]	C-terminus	Structure [b] % helicity	Peptide-lipid binding selectivity [c] PCPS/PC	Stability [d] % peptide 24 h	Activity [e] Pf IC_{50} (μM) Ser + Alb	Activity [e] Pf IC_{50} (μM) Alb	Hemolysis [f] HC_{10} (μM)	Activity-hemolysis index [g] RBC HC_{10}/Pf IC_{50}
ref [30]	1	no G1	amide	43	2.4	65.4 ± 3.4	16.9 ± 1.1	12.5 ± 0.8	105.3 ± 2.9	8.4 ± 0.8
ref [35]	2	no G1; del C2, E35, S36	thioether, amide	41	2.3	66.0 ± 2.5	~40	~8	nd	na
ref [36]	3		amide	50	3.0	53.7 ± 3.9	11.9 ± 0.9	13.6 ± 1.7	>128	>9
AA position / peptide 3		1 2 3 12345678901234567890123456789012345 6 GCGGPLYKKIIKKLLESGGSGGAPLYKKIIKKLCES-NH_2								
Set 1. substituted charged or hydrophobic residues	4	deleted E35, S36	ΔES, amide	36	2.4	10.4 ± 0.1	12.3 ± 1.0	**6.4 ± 0.2**	25.7 ± 2.1	4.0 ± 0.5
	5	K8R, K27R	ΔES, amide	54	3.0	0	11.3 ± 0.7	**5.0 ± 0.2**	22.8 ± 1.9	4.6 ± 0.6
	6	K9R, K28R	ΔES, amide	50	2.3	3.6 ± 2.3	12.3 ± 1.0	**4.5 ± 0.1**	34.1 ± 4.8	7.6 ± 1.2
	7	K12R, K31R	ΔES, amide	45	2.3	5.6 ± 0.2	11.2 ± 0.6	**5.1 ± 0.2**	28.2 ± 4.1	5.5 ± 1.0
	8	K13R, K32R	ΔES, amide	48	2.8	11.5 ± 0.1	10.4 ± 0.7	**4.8 ± 0.1**	50.1 ± 3.9	**10.4 ± 1.0**
	9	all K to R	ΔES, amide	43	2.5	4.4 ± 0.2	12.5 ± 1.2	**4.8 ± 0.2**	6.6 ± 0.9	1.4 ± 0.2
	10	E16K	ΔES, amide	33	2.3	0	11.8 ± 1.2	**2.3 ± 0.1**	14.9 ± 2.1	6.5 ± 1.2
	11	K12R, E16K, K31R	ΔES, amide	40	2.0	1.2 ± 0.1	16.4 ± 2.0	**3.2 ± 0.2**	6.3 ± 1.0	2.0 ± 0.4
	12	E16K	amide	34	2.0	0	12.5 ± 1.1	**5.0 ± 0.1**	34.9 ± 5.5	7.0 ± 1.2
	13	E16K, E35K	amide	26	2.0	0	10.2 ± 0.6	**3.7 ± 0.2**	6.3 ± 1.0	1.8 ± 0.5
	14	I11V, I30V	ΔES, amide	27	1.7	17.4 ± 1.0	~45	12.7 ± 0.7	~52	~4
	15	L14H, S17R, L33H	ΔES, amide	14	2.3	0	>>67.5	>>67.5	>128	na
	16	Y7W, Y26W	ΔES, amide	43	2.3	53.6 ± 4.9	3.0 ± 0.2	**2.2 ± 0.1**	8.4 ± 0.8	3.8 ± 0.5
Set 2. modified C-terminus	17	Del E35, S36	ΔES, carboxyl	21	nd	4.9 ± 0.1	>67.5	19.3 ± 1.1	74.7 ± 3.5	3.9 ± 0.4
	18	G4A	amide	37	2.5	52 ± 4.9	26.2 ± 1.7	15.3 ± 0.9	14.7 ± 1.3	1.0 ± 0.1
	19		carboxyl	35	1.7	**66.1 ± 5.0**	34.3 ± 3.2	21.6 ± 1.4	>128	>6
	20		backbone cyclic	21	1.9	**58.6 ± 1.5**	37.6 ± 3.4	26.3 ± 1.9	95.7 ± 3.5	3.6 ± 0.4
	21	S36N	backbone cyclic	15	2.2	**73.7 ± 6.9**	~27	~46	>128	>3
	22	E35Q, S36N	backbone cyclic	23	2.1	22.5 ± 3.5	24.7 ± 3.0	19.1 ± 1.9	>128	>7
	23	E35K, S36N	backbone cyclic	37	2.1	40.5 ± 4.3	14.4 ± 1.3	13.1 ± 1.0	22.1 ± 2.4	1.7 ± 0.3
	24	+ GGSGG linker, no ds	backbone cyclic	35	1.9	**88.8 ± 2.8**	9.0 ± 1.3	**7.9 ± 0.8**	92.7 ± 10.9	**11.7 ± 2.6**
	25	linker, no ds, S17N, S36N	backbone cyclic	17	1.9	24 ± 0.3	8.7 ± 0.7	**6.3 ± 0.7**	79.9 ± 8.3	**12.7 ± 2.7**
Combined	26	linker, no ds, E16K	backbone cyclic	24	2.4	12.2 ± 1.0	9.2 ± 1.0	**3.5 ± 0.4**	~100	**~30**
	27	linker, no ds, K13R, K32R	backbone cyclic	21	2.2	**75.8 ± 1.1**	12.5 ± 0.9	**5.3 ± 0.4**	17.7 + 3.9	2.8 ± 0.9

[a]Sequence change relative to peptide **3**, with the full amino acid sequence shown in Table S1; ds, disulfide bond. [b]% helicity was determined from the lowest MRE between 218 and 222 nm for 50 μM peptide in 100 mM NaF, 10 mM KH_2PO_4, pH 7.5 (Figures 4A, 5A, 6A). [c]Relative peptide binding PCPS/PC was determined using P/L at the end of the association phase of 16 μM peptide bound to POPC/POPS (4:1) compared to POPC bilayers (Figure 4C, 5C, 6C). [d]% peptide remaining was determined from area under the curve of the $[M + 4]^{4+}$ peak (intact mass) using TOF-MS. Peptide analogues (50 μM) were incubated in 25% (v/v) serum in PBS at 37 °C for 24 h and compared to 0 h controls (100% peptide). [e]Pf IC_{50}, peptide concentration to inhibit 50% growth of *P. falciparum* 3D7 compared to untreated controls, as determined from dose−response curves (Figure S5). Growth inhibition was determined from DAPI staining of parasite nuclei after 72 h incubation at 37 °C, 5% CO_2, 5% O_2. Culture medium was supplemented with either 5% serum, 2.5 mg/mL Albumax II (Ser + Alb), or 5 mg/mL Albumax II (Alb). [f]Hemolysis HC_{10}, peptide concentration that lyses 10% of uninfected RBCs, determined from dose−response curves for released hemoglobin (Figure S6). Less than 10% hemolysis was confirmed within the active concentration range for **3**, **10**, **12**, **24**, and **26** up to 72 h incubation. [g]Activity-hemolysis index comparing 50% inhibition of *in vitro P. falciparum* (5 mg/mL Albumax II supplement) to 10% hemolysis of uninfected RBCs. Values highlighted in bold indicate improvements over the respective scaffold peptides (**1**−**3**).

and mass data for the base scaffolds and analogues (**4**−**27**) are shown in Table S1, with purity demonstrated in Figures S1 and S2. The % helicity (structure), stability in the presence of serum proteases, *in vitro* activity against *P. falciparum*, hemolysis, and activity-hemolysis index between antiplasmodial activity and RBC lysis are summarized in Table 1.

Peptide Set 1: Substitution of Charged and Hydrophobic Residues. *Design.* The peptide scaffold used as the base for set 1 analogues was ctPF4PD (**2**), a variant of cPF4PD

https://doi.org/10.1021/acsinfecdis.4c00276
ACS Infect. Dis. 2024, 10, 2899−2912

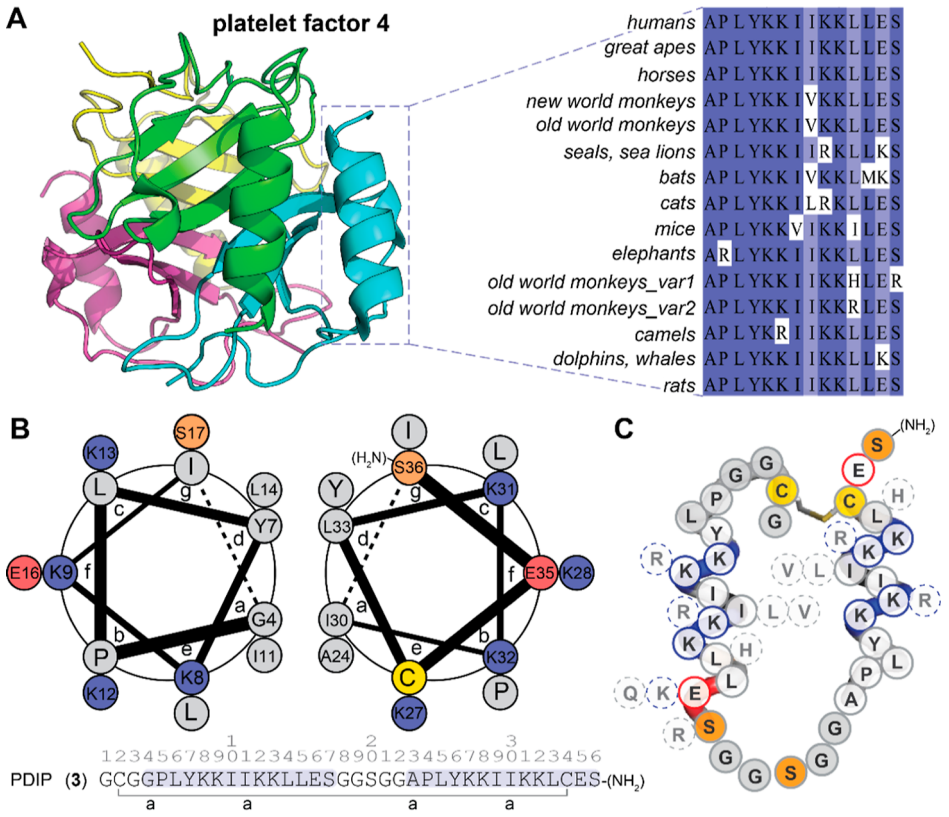

Figure 3. Sequence Diversity of the C-terminal 14 Amino Acids of PF4 Informed the Design of PDIP Analogues. (A) C-terminal 14 amino acids of PF4 subunits (PDB: 1F9Q) arrange into paired α-helices. Representative sequence of PF4 C-terminal amino acids showing naturally occurring substitutions (full alignment from BLASTP search of nonredundant protein sequences is shown in Figure S3). (B) Helical wheel diagram showing the predicted position of residues in the two helices of PDIP analogue **3**; heptad position is shown (a−g), and the diagram was generated using DrawCoil 1.0 (https://grigoryanlab.org/drawcoil). (C) A cartoon of PDIP (**3**) shows the location of amino acid substitutions.

(**1**) with a truncated C-terminus (Glu, Ser deleted; ΔES), C-terminal amide, and a thioether linkage replacing the disulfide bond. We had previously demonstrated similar properties between **1** and **2**[35] and proposed that the shorter scaffold would be more desirable for drug development. In other work, we added a Gly to the N-terminus to produce disulfide macrocyclic peptide **3**,[36] with improved ability to use the Cys residue for covalent bridge formation if required (e.g., acetone staple).[37] Therefore, we maintained N-terminal Gly in the newly designed C-terminally truncated, disulfide macrocyclic analogues. To select residues for substitution in set 1, we examined the natural sequence diversity within the C-terminal region of PF4 subunits by performing a BLASTP search (https://blast.ncbi.nlm.nih.gov)[38] of a nonredundant protein database (Figure S3). The representative sequence variants shown in Figure 3A were transposed onto the PDIP scaffold (Figure 3B,C) to produce analogues **4**−**16**. We were interested in determining whether replacing Lys with Arg (**5**−**9**) or increasing the overall charge (**10**) would promote stronger interactions with negatively charged membranes and thereby increase potency against malaria parasites. Substitutions to inward facing hydrophobic residues (see Figure 3B) were included to determine the effect on membrane interaction for peptides with the shorter side chain of Val (**14**) in place of Ile in the parent sequence or the bulkier side chain of Trp (**16**) replacing Tyr in the base sequence. Previous studies have demonstrated that replacing Tyr with Trp and/or Lys with Arg can improve the membrane-binding affinity of AMPs without increasing non-selective binding or toxicity.[39,40] Dual substitutions in **11** and **15** were included due to their natural occurrence in PF4 from nonhuman species. Peptides **12** and **13** were included to determine the effect of the charge reversing Glu-to-Lys substitution on the full-length peptide **3** scaffold.

Structure and Stability. We previously demonstrated that cPF4PD (**1**) maintains a helical structure in aqueous solution, which likely explains its increased resistance to breakdown by serum proteases and improved activity against *P. falciparum* parasites compared to a linear 14 amino acid peptide from PF4's C-terminus.[28,30] To determine whether these desirable characteristics were maintained for the peptides in the present study, we examined their structure using circular dichroism (CD) spectroscopy (Figure 4A) and calculated the % helicity (shown in Table 1) from the minimal mean residual ellipticity (MRE) (218−222 nm) of the peptides in aqueous solution (100 mM NaF, 10 mM KH_2PO_4 pH 7.5). The CD spectra observed for parent peptides **1**−**3** confirmed an overall helical structure with spectral minima at 208 and 222 nm. Lys-to-Arg-substituted peptides **5**−**9** had similar % helicity to **3**, but the new truncated scaffold peptide (**4**) and Glu-to-Lys-substituted peptides **10**−**13** were less helical. Ile-to-Val substitution in **14** decreased the % helicity to a similar extent, whereas Tyr-to-Trp substitution in **16** had less effect on helix formation. The CD spectrum for **15** was consistent with a random coil structure, suggesting that the Leu-to-His substitutions on the inward-facing region of the helices completely disrupted helix formation in the tested aqueous solution (see Figure 4A and Table 1). We also examined the CD spectrum for **15** under more acidic conditions (pH 5) as some AMPs with a His residue undergo pH-dependent changes in

https://doi.org/10.1021/acsinfecdis.4c00276
ACS Infect. Dis. 2024, 10, 2899−2912

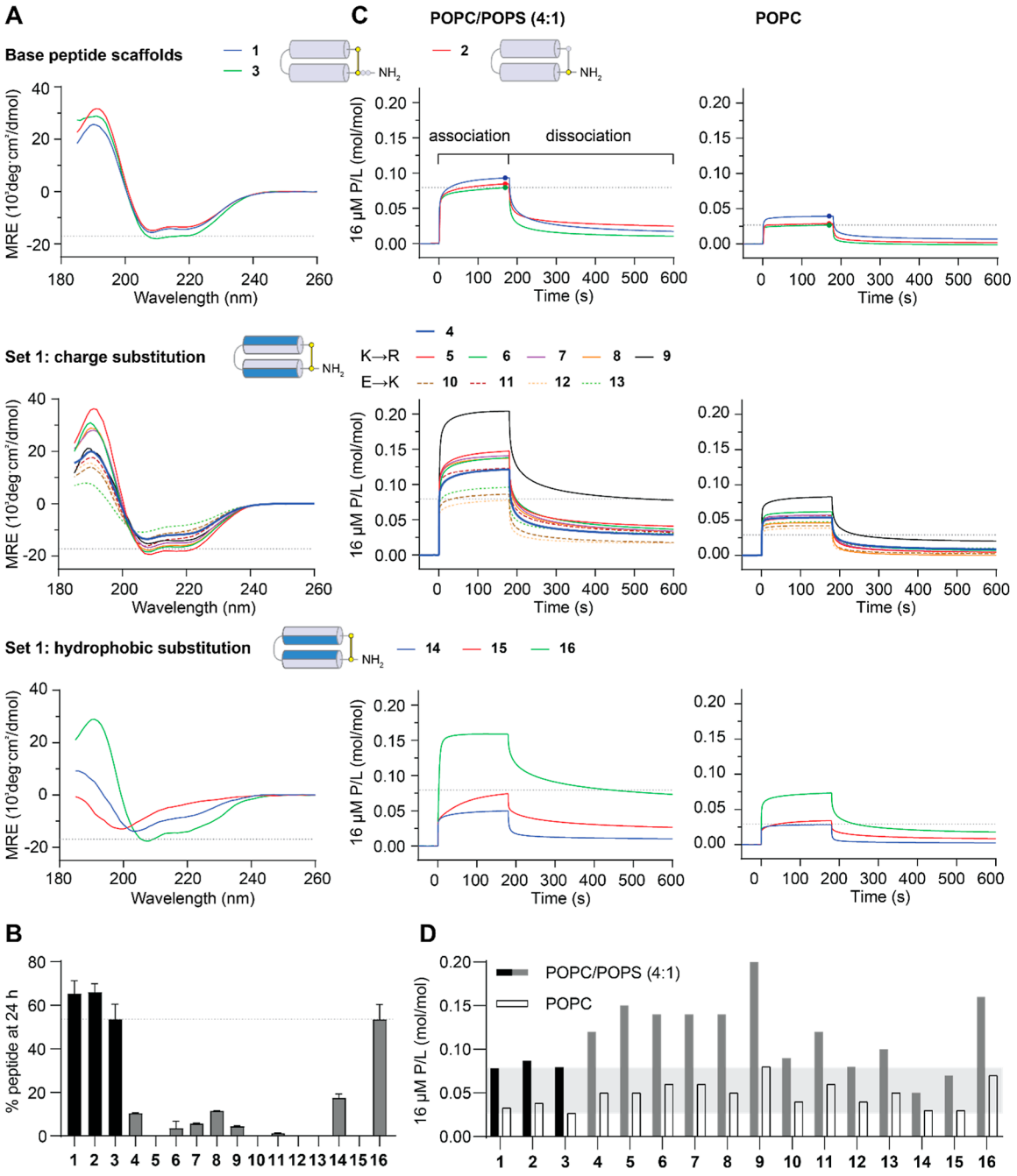

Figure 4. Characteristics of PDIP Base Peptides and Set 1 Analogues. (**A**) CD spectra were collected for 50 μM peptides in aqueous solution (100 mM NaF, 10 mM KH_2PO_4 pH 7.5). Peptides with spectral minima at 208 and 222 nm have an overall helical structure. The MRE at 222 nm was used to calculate percentage helicity (Table 1). (B) Resistance to breakdown by serum proteases was determined from the amount of peptide remaining after 24 h of incubation with 25% (v/v) human serum. Peptides were quantified relative to time zero samples from area under the curve of intact mass m/z peaks using TOF-MS. (C) Peptide−lipid binding was compared using surface plasmon resonance (SPR) sensorgrams collected for 16 μM peptides binding to POPC/POPS (4:1) and POPC lipid bilayers. Response units (RU) were converted to P/L using $(RU_{peptide}/mw_{peptide})/(RU_{lipid}/mw_{lipid})$. P/L at the end of the association phase (170 s) was used for comparing the peptide−lipid binding affinity for POPC/POPS (4:1) compared to that of POPC membranes in (D) (Table 1). Dashed lines or shaded regions provide a comparison to peptide **3** in each of the plots. Structure cartoons show the location of substitutions (in blue) relative to the parent scaffold.

structure that confer differences in membrane-permeabilizing properties[41] as well as in a less polar solvent mixture (50% trifluoroethanol, TFE) to determine whether helix formation occurs in more hydrophobic environments, akin to membrane interactions (Figure S4A). pH-dependent changes were not observed for **15** or parent peptide **2**, included as the scaffold control, and **15** adopted a similar helical structure to **2** in 50% TFE, suggesting that the substituted residues did not hinder the propensity to form α-helices in more hydrophobic environments. Overall, set 1 analogues with Lys-to-Arg substitution (**5**−**9**) had similar helicity in aqueous solution to parent peptides **1**−**3**, whereas Glu-to-Lys substitution (**10**−**13**) adversely affected helicity. Substitution of hydrophobic residues (Ile-to-Val, **14**;

https://doi.org/10.1021/acsinfecdis.4c00276
ACS Infect. Dis. 2024, 10, 2899−2912

Leu-to-His, **15**) had the strongest adverse effect on helicity in an aqueous solution.

To investigate proteolytic stability, we used time-of-flight mass spectrometry (TOF-MS) to determine the amount of peptide remaining after incubation with a protease-rich solution of 25% human serum (v/v) in phosphate buffered saline (PBS) for 24 h at 37 °C, relative to 0 h controls (100% for each peptide). The 24 h time point was chosen to compare all analogues in this study as it is close to the half-life for parent peptide **1** in these conditions.[30] Most of the peptides in set 1 had lower serum stability compared to that of scaffold peptides **1**−**3**, suggesting that removal of C-terminal Glu and Ser residues, without the thioether linkage present in **2**, adversely affects the stability (Figure 4B, Table 1). Peptides with Glu-to-Lys substitutions (**10**−**13**) were the least stable. Peptide **16** (Tyr-to-Trp substitution) was the most stable set 1 analogue, having similar stability to the parent scaffolds.

Interaction with Lipid Bilayers. The ability of cPF4PD (**1**) to preferentially bind to and lyse membranes that are rich in negatively charged phospholipids contributes to its selective entry into infected RBCs and subsequent lysis of parasite digestive vacuole membranes.[30] This selectivity was therefore a beneficial characteristic that we wished to maintain in the analogues. In the current study, we use SPR to compare the binding interactions between each peptide and two different lipid bilayers. One was composed of neutral palmitoyl-2-oleoyl-*sn*-glycero-3-phosphocholine (POPC) to mimic the properties of the outer leaflet of healthy uninfected RBC. The other contained a mixture of POPC with 1-palmitoyl-2-oleoyl-*sn*-glycero-3-phosphoserine (POPS) in a 4:1 ratio (POPC/POPS 4:1) to mimic the properties of *P. falciparum*-infected RBCs, in which negatively charged PS headgroups are exposed on the outer leaflet of the host cell membrane (Figure 1A).[19,20] This method reports on relative binding but not whether peptides penetrate or lyse the different lipid bilayers. However, we previously demonstrated excellent correlation between relative binding to lipid bilayers and lysis of vesicles comprising similar lipid mixtures for peptides **1** and **2**.[30,35]

Figure 4C shows the rapid association and dissociation of peptides **1**−**3**, with a higher P/L (ratio of peptide binding to lipid) obtained for POPC/POPS (4:1) compared to that obtained for POPC lipid bilayers, indicating the selective binding of these peptides to negatively charged compared to neutral membranes. Set 1 peptides showed similar rapid association and dissociation characteristics, except **14** (Ile-to-Val substitution), which had a slower association with POPC/POPS (4:1) bilayers. P/L values at the end of the association phase for 16 μM peptides were used to provide a comparison between relative binding to bilayers (see Figure 4D, and relative binding of POPC/POPS (4:1):POPC reported in Table 1). These values demonstrate the maintained selectivity between POPC/POPS (4:1) and POPC bilayers for all set 1 peptides. Most of the analogues with charge substitutions (**5**−**13**), together with **16** (Tyr-to-Trp substitution), had higher binding affinity (higher P/L values) for POPC/POPS (4:1) bilayers than scaffold peptides **1**−**3**. However, the affinity for POPC bilayers was also increased for these peptides, suggesting that the increase was not completely selective.

Antiplasmodial Activity and Activity-Hemolysis Index. Despite the lower serum stability observed for set 1 analogues, we remained interested in examining whether the substitutions affect *in vitro* growth of *P. falciparum*. Therefore, we performed activity experiments in the presence (culture medium supplemented with 5% serum, 2.5 mg/mL Albumax II; Ser + Alb) or absence (5 mg/mL Albumax II; Alb) of human serum. This assay was performed in a 384-well plate format, and growth inhibition was determined after 72 h based on the detection of DAPI-stained parasite nuclei using automated analysis.[42,43] As anticipated, dose−response curves for set 1 peptides showed enhanced inhibition of parasite growth when serum was excluded from the experiment, whereas parent peptides **1** and **3** had similar curves in both conditions (Figure S5). Peptide concentrations required to inhibit 50% of *P. falciparum* growth (IC_{50}) were determined from the dose−response curves and are summarized in Table 1 for both assay conditions. To allow distinction between antiplasmodial activity and nonselective lysis of RBCs, the hemolytic activity of the analogues was determined by measuring the release of hemoglobin following incubation of peptides with uninfected RBCs. Peptide concentrations required to lyse 10% of RBCs (HC_{10}) were determined from dose−response curves (Figure S6) and are summarized in Table 1.

An activity-hemolysis index (*P. falciparum* IC_{50} relative to RBC HC_{10}) was calculated for the analogues, as summarized in Table 1, and used to assess their relative selectivity for parasite killing over RBC lysis. Analogues with higher activity-hemolysis index values were considered the most desirable.

From the parasite activity assays, truncated scaffold peptide **4** and charge variant peptides **5**−**13** showed between two- and six-fold enhancement in potency against *P. falciparum* in the serum-free experiments, consistent with their higher affinity for binding to negatively charged POPC/POPS (4:1) bilayers (see Figure S7). However, hemolysis was also increased for most of these peptides, and the activity-hemolysis index between *P. falciparum* IC_{50} and RBC HC_{10} observed for parent peptides **1** and **3** (8.4 −>9) was only maintained for charge-substituted peptide **8** (see Table 1). Interestingly, this peptide has similar Lys-to-Arg substitutions compared to **5**−**7**, suggesting that positioning of the substituted Arg closest to Glu16 (Figure 3B) is best suited for improving membrane penetration without increasing nonselective disruption.

Substitution of inward-facing Ile or Leu residues adversely affected parasite growth inhibition. Ile-to-Val substitution (**14**) resulted in a two-fold decrease compared to parent scaffold peptide **2**, and Leu-to-His (polar at neutral pH, positive charge at acidic pH e.g. inside the *P. falciparum* digestive vacuole) substitution resulted in no parasite killing detected for **15** up to 67 μM. For both peptides, the lower activity was consistent with decreased helicity in aqueous solution and increased susceptibility to breakdown by serum proteases. However, the loss of *P. falciparum* growth inhibition is not explained by diminished membrane interaction (see Figure 4D) or selective uptake into infected versus uninfected RBCs (see Figure S4B) as **15** performed similarly to parent peptides **1**−**3** with respect to these parameters. These observations, together with the ability of **15** to adopt a helical structure in a less polar solution with 50% TFE (see Figure S4A), suggest that the helical regions of **15** become structured when encountering membranes of infected RBCs, thereby facilitating cell penetration. The loss of activity against the intracellular target(s) remains unexplained. Substitution of Tyr with Trp (**16**) produced the most stable truncated analogue, with the most potent activity against *P. falciparum*. However, like the charge-inverted (Glu-to-Lys) peptide **10**, the activity-hemolysis index between antiplasmodial activity and hemolysis of RBCs was decreased compared to parent scaffold peptides **1** and **3** (Table 1).

https://doi.org/10.1021/acsinfecdis.4c00276
ACS Infect. Dis. 2024, 10, 2899−2912

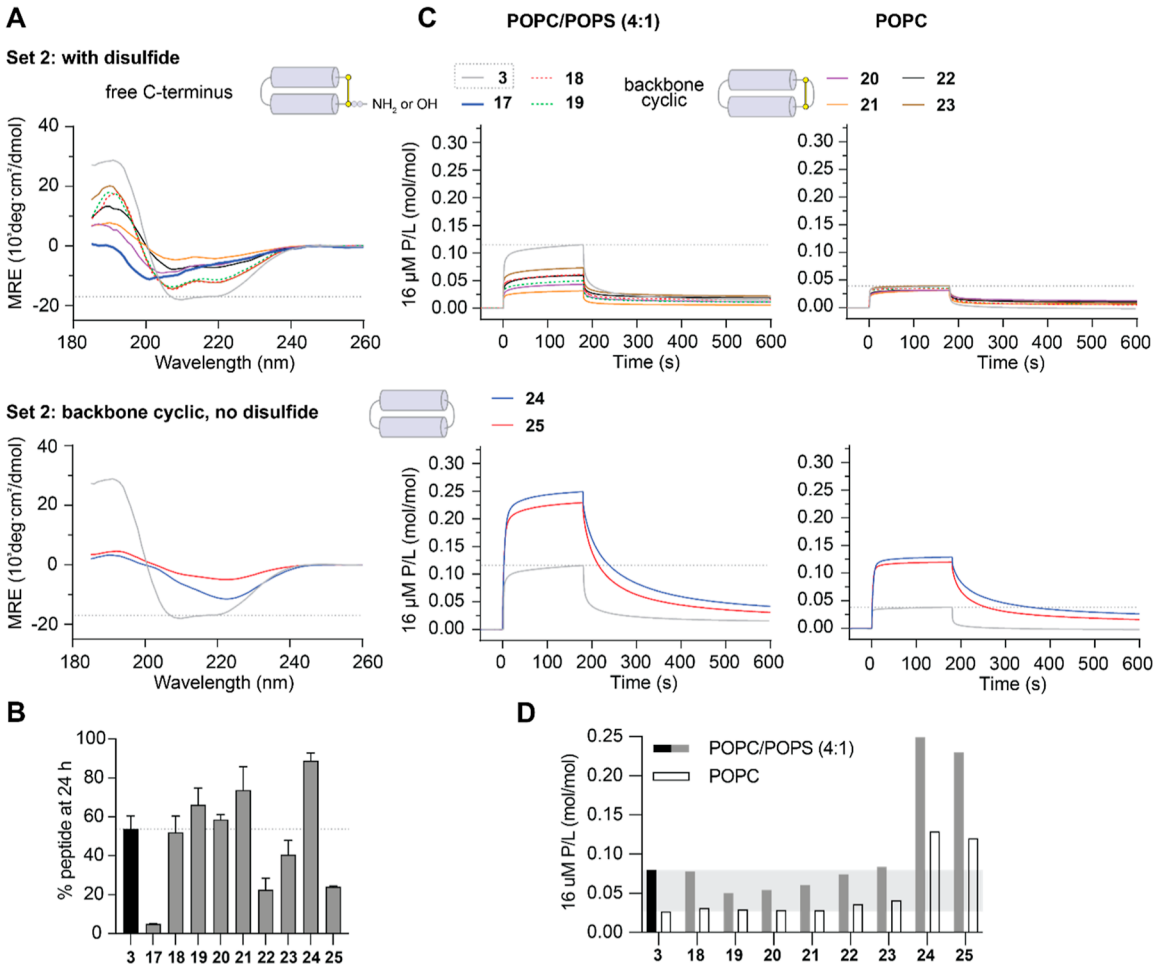

Figure 5. Characteristics of Set 2 Analogues. (A) CD spectra were collected for 50 μM peptides in aqueous solution (100 mM NaF, 10 mM KH_2PO_4 pH 7.5) as above. (B) Resistance to breakdown by serum proteases was determined from the amount of peptide remaining after 24 h incubation with 25% (v/v) human serum as above. (C) Peptide−lipid binding was compared using SPR sensorgrams collected for 16 μM peptides binding to POPC/POPS (4:1) and POPC lipid bilayers as above. P/L at the end of the association phase (170 s) was used for comparing peptide−lipid binding affinity for POPC/POPS (4:1) compared to POPC membranes in (D). Peptide **3** is included, with dashed lines or shaded regions providing a comparison in each of the plots.

Peptide Set 2: Modification of Peptide C-Terminus. *Design.* Encouraged by the ability to improve potency against *P. falciparum* by substituting amino acid residues, we next sought to improve peptide stability with a focus on maintaining compatibility for the biosynthetic production of lead peptides. Peptides **17** and **19** were included to determine whether the C-terminal amide could be replaced by a carboxylic acid (akin to biosynthetic products), and **18** served as a control peptide for replacing Gly4 in the peptide **3** scaffold with Ala, the conserved amino acid at this position in PF4 (Figure S3). Cyclization is known to improve peptide stability,[44,45] and peptide ligation can be achieved in biosynthetic pathways using asparaginyl endopeptidase (AEP) enzymes that leave a minimal Asn footprint in the resultant cyclic peptide.[46,47] Peptides **20**−**23** were included to examine the effect of backbone cyclization of the peptide **3** scaffold (**20**) (compared to macrocyclization exclusively via the disulfide bridge), introduction of Asn into the sequence (**21**), and replacement of negatively charged Glu with Gln (**22**) or Lys (**23**). Peptides **24** and **25** contain a flexible linker (GGSGG) in place of the disulfide bond, with Ser-to-Asn substitution additionally explored in **25**.

Structure and Stability. Disulfide-bridged macrocycles with modified C-terminal residues (**17**−**19**) and backbone cyclic peptides with a retained disulfide bond (**20**−**23**) had an overall helical structure in aqueous solution, albeit with reduced % helicity compared to scaffold peptides **1**−**3**. However, the CD spectra of backbone cyclic peptides with a flexible linker between the helices but no disulfide bond (**24**−**25**) suggested a deviation from a well-defined helical structure (Figure 5A).

Proteolytic stability was maintained or improved compared to scaffold peptides (**1**−**3**) for all set 2 peptides, except for truncated peptide **17**, which has a C-terminal carboxylic acid, and **22** and **25**, which have both Gln and Asn substitutions or contain two Asn residues (Figure 5B). The stability of backbone cyclic analogues with a single Asn substitution (**21** and **23**) suggests that this inclusion is well tolerated, which is a promising outcome for future cyclization of peptides using AEP ligases during biosynthetic production.

Interaction with Lipid Bilayers. Replacement of the C-terminal amide with a carboxylic acid in **19** or through backbone cyclization in **20** lowered the binding affinity for both tested lipid bilayers, but this was partly overcome by including Asn in the peptide sequence for backbone cyclic peptides **22** and **23**. Replacement of the disulfide bond with a flexible GGSGG linker in backbone cyclic peptides **24** and **25** increased the overall membrane binding affinity (Figure 5C) and retained selectivity

https://doi.org/10.1021/acsinfecdis.4c00276
ACS Infect. Dis. 2024, 10, 2899−2912

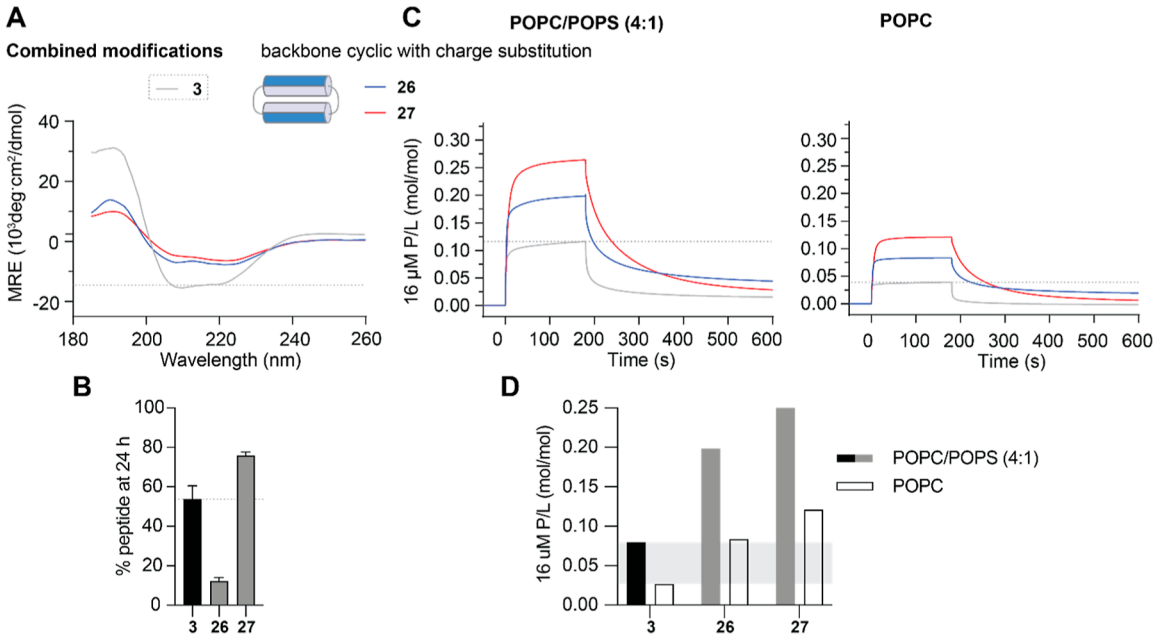

Figure 6. Characteristics of PDIP Analogues with Combined Modifications. (A) CD spectra were collected for 50 μM peptides in aqueous solution (100 mM NaF, 10 mM KH_2PO_4 pH 7.5) as above. (B) Resistance to breakdown by serum proteases was determined from the amount of peptide remaining after 24 h incubation with 25% (v/v) human serum as above. (C) Peptide−lipid binding was compared using SPR sensorgrams collected for 16 μM peptides binding to POPC/POPS (4:1) and POPC lipid bilayers as above. P/L at the end of the association phase (170 s) was used for comparing peptide−lipid binding affinity for POPC/POPS (4:1) compared to POPC membranes in (D). Peptide **3** is included, with dashed lines or shaded regions providing comparison in each of the plots.

for negatively charged POPC/POPS (4:1) compared to neutral POPC bilayers (Figure 5D). One explanation for the increased affinity of **24** and **25** is that some of the inward-facing hydrophobic residues become more surface exposed due to their more conformationally flexible and less-defined structure compared to that of the parent peptides (Figure 5A).

Antiplasmodial Activity and Activity-Hemolysis Index. Consistent with their superior serum stability profiles, set 2 peptides (except for truncated **17**) had more similar IC_{50} values for *P. falciparum* growth inhibition in the presence or absence of serum in culture medium compared to set 1 analogues (Figure S5, Table 1). However, modification of the C-terminus (including carboxylic acid or backbone cyclization) of the peptide **3** scaffold (peptides **18**−**23**) decreased the antiplasmodial potency. It is possible that increased structural rigidity combined with insufficient spacing between the joined N- and C-terminal residues of backbone cyclic peptides **20**−**23** caused an unfavorable presentation of residues at positions 35 and 36. Inclusion of a longer flexible linker between the terminal residues appeared to restore full peptide function, and consistent with the observed increase in membrane-binding affinity (Figure 5C), **24** and **25** had increased potency (lower IC_{50}) for inhibiting *P. falciparum* growth. These analogues maintained selectivity for negatively charged membranes (Figure 5D) and had an activity-hemolysis index at least as high as that of the parent scaffold peptide **3** (Table 1). Together, these results show that backbone cyclized PDIP analogues with extended linkers between the two helices have superior ability to resist breakdown by serum proteases, maintain selectivity for negatively charged lipids, and have enhanced ability to kill *P. falciparum* parasites *in vitro*.

Combined Potency-Enhancing Substitutions and Stability-Enhancing Modifications. *Design.* The most promising potency-enhancing substitutions (E16K; and K13R, K32R) identified from set 1 analogues were incorporated onto the most stable and selective peptide scaffold (**24**) identified from set 2 analogues to produce **26** and **27**, respectively.

Structure and Stability. Both **26** and **27** had a helical structure in aqueous solution (Figure 6A), but with a lower % helicity than the corresponding charge-substituted disulfide macrocyclic analogues (**10**−**13** with E16K; **8** with K13R, K32R) or backbone cyclic scaffold peptide **24** (see Table 1). The observed changes in % helicity did not appear to affect stability as resistance to breakdown by serum proteases was improved for charge-substituted backbone cyclic analogues compared to their disulfide macrocyclic counterparts. After 24 h of incubation in 25% (v/v) serum in PBS, 12% of **26** remained compared to 0% for **10**−**13**, and 76% of **27** remained compared to 12% of **8** (Figures 5B and 6B).

Interaction with Lipid Bilayers. Peptides **26** and **27** had similar high peptide-to-lipid binding ratios (P/L) as scaffold peptide **24** and maintained selectivity for negatively charged POPC/POPS (4:1) compared to neutral POPC lipid bilayers (Figure 6C,D and Table 1).

Antiplasmodial Activity and Activity-Hemolysis Index. Introducing the E16K substitution onto a stable backbone cyclic scaffold (**26**) resulted in similar increased *in vitro* activity against *P. falciparum* (IC_{50} 3.5 μM), as observed for disulfide macrocyclic counterparts, but with greatly improved activity-hemolysis index between antiplasmodial activity and RBC lysis, and HC_{10} > 100 μM for **26** (Table 1). The potency enhancement observed for the K13R, K32R substitution (disulfide macrocyclic peptide **8**) was also maintained on the stable backbone cyclic scaffold (IC_{50} 5.3 μM for **27** compared to 4.8 μM for **8**, no serum condition). However, this combination produced a more hemolytic peptide with an RBC HC_{10} of 18 μM for **27** (Table 1).

https://doi.org/10.1021/acsinfecdis.4c00276
ACS Infect. Dis. 2024, 10, 2899−2912

DISCUSSION

New antimalarial candidates need to overcome many challenges as they progress along the drug development pipeline. Ideally, they kill *Plasmodium* parasites at multiple life cycle stages, are inexpensive and easy to administer, are effective against most circulating drug-resistant strains, and have a good resistance profile.[2] We propose that peptide-based drugs have the potential to fulfill these requirements. In addition, the different mechanism of action of PF4-derived peptides compared to that of current antimalarial drugs makes them useful candidates for development as drug partners in new combination therapies.

Peptide scaffolds can be modified to enhance the structural stability and resistance to breakdown. We reasoned that improving PDIP resistance to proteolytic breakdown would enhance antiplasmodial potency by having the active peptide present for a longer treatment time. Backbone cyclization of PDIP analogues with flexible linkers between the two bioactive helical sequences produced a more stable scaffold (**24**), although we observed a deviation away from the overall helical structure of parent peptides **1**−**3**. Three of the four peptides with this less-defined structure (**24**−**26**) had improved antiplasmodial potency and favorably low hemolytic activity compared to the parent peptides, but future scaffold adaptations that promote peptide helical structure in aqueous solution (e.g., reintroduction of a disulfide bond between the paired helices) might be required.

Peptides can be readily modified by substituting amino acids in the primary sequence. However, careful consideration of the locations of target residues is required. Here, we demonstrate that changes to inward-facing hydrophobic residues of the PDIP scaffold likely induced structural changes that decreased potency against *P. falciparum* (**14** and **15**). Conversely, changes to outward-facing charged residues (**5**−**13**) did not noticeably alter the helical structure and enhanced antiplasmodial potency, but many of these also increased the hemolysis of uninfected RBCs. Two promising substitutions were identified, E16K (**10**, **12**) and K13R, K32R (**8**), that enhanced antiplasmodial potency and maintained a good activity-hemolysis index. However, both substitutions produced less proteolytically stable peptides compared with scaffold peptides **1**−**3**.

Our approach of combining these desirable potency-enhancing substitutions onto the most stable cyclic peptide scaffold (**24**) was successful in producing an analogue (**26**, E16K substitution) that satisfied the requirements of enhanced antiplasmodial potency and low hemolytic activity compared to first generation peptides (**1**−**3**). Backbone cyclic analogue **26** had improved resistance to serum proteases compared to charge-inverted disulfide macrocyclic counterparts (**10**−**13**), but further improvement in stability is required for the progression of **26** as a drug candidate. There are several examples of helical peptides where substitution of Lys or Arg residues proximal to the C-terminus with their D-amino acid counterparts improves resistance to proteolytic breakdown while maintaining overall helical structure and bioactivity.[48−50] Incorporation of D-Lys in positions 16 or 36 of the PDIP scaffold may provide similar benefits, but this approach would deviate from our current efforts to maintain an all-L-amino-acid scaffold to allow transfer to a biosynthetic production pathway.

Toward the goal of future biosynthetic production, we explored whether deviation from the C-terminal amide of first-generation PDIP analogues would affect the overall properties and bioactivity. Disulfide macrocyclic analogues with a C-terminal carboxylic acid (**17**, **19**) and backbone cyclic analogues with a maintained disulfide bond (**20** and **21**) had lower antiplasmodial activity, but this was partially recovered by altering the charge at C-terminal position 35 from negative (Glu) to neutral polar (Gln, **22**) or positive (Lys, **23**). Notably, **21**−**23** also contained an Asn residue, confirming that this residue is well tolerated in the backbone cyclic PDIP scaffold. This is an important requirement for incorporating AEP enzymatic cyclization into biosynthetic production methods.[46,47]

The cost of new antimalarial drugs is a major hurdle to overcome as the regions most affected by the disease have the poorest economies and out-of-pocket treatment costs are prohibitive for low-income earners (recently reviewed[51,52]). Efforts to reduce the cost of antimalarial drugs include improvements in synthesis efficiency (e.g., artemisinin biosynthesis[53,54]) and promotion of local manufacture to bypass expenses incurred by import and distribution.[55] Likewise, the cost of producing and distributing peptides is a limitation that must be addressed when developing peptide-based therapeutics. Toward this requirement, we and others are optimizing biosynthetic methods for producing therapeutic peptides.[56−58] Importantly, disulfide-rich cyclic peptides can be produced with high yields via yeast[57] or plant[59,60] expression systems. Production and recovery of biosynthetic products is less expensive, requires simpler infrastructure, and is more environmentally friendly than chemical synthesis,[57] making it amenable for local production as a means of further reducing costs.

Challenges that we have not addressed in this study include the determination of activity against drug-resistant *P. falciparum*, activity against other life cycle stages, and evaluation of resistance risk. Here, we examined the *in vitro* activity against blood-stage parasites of the drug-sensitive *P. falciparum* 3D7 strain. Studies on drug-resistant strains will be required, but we anticipate similar activity against drug-sensitive and -resistant strains due to the differences in the mechanism of action between PDIP and small-molecule antimalarial drugs[2,30] and because the parental PF4 protein, which acts on parasites via the same membrane-active mechanism,[28] is equally active on drug sensitive and resistant strains.[27] In other work (unpublished), we are examining the effect of PDIP and PDIP-drug conjugates[36] on the development of sexual-stage gametocytes and maturation into macrogametes.[61] Measuring resistance risk is a challenging undertaking, requiring culture of *P. falciparum* under drug pressure for long periods of time, especially if the parasites are refractory to developing resistance to the target drug.[2] On the basis of previous resistance studies with AMP-treated bacteria[62] and our observations with melanoma cells (peptide versus dabrafenib acquired resistance),[63] we anticipate a slower acquisition of resistance to peptides, and with a greater fitness cost to *Plasmodium* parasites compared to small-molecule drugs.

CONCLUSIONS

Here we describe the rational optimization of the selective, membrane-active PDIP scaffold. We identified an antiplasmodial potency-enhancing substitution (E16K) and incorporated this into a stable and selective scaffold (**24**) to produce a backbone cyclic PDIP analogue (**26**) with low micromolar activity against *in vitro P. falciparum* parasites (see Figure 7). The outcomes of this study represent a practical advance in developing the PDIP scaffold as an antimalarial molecule and provide a framework for monitoring and selecting desirable

https://doi.org/10.1021/acsinfecdis.4c00276
ACS Infect. Dis. 2024, 10, 2899−2912

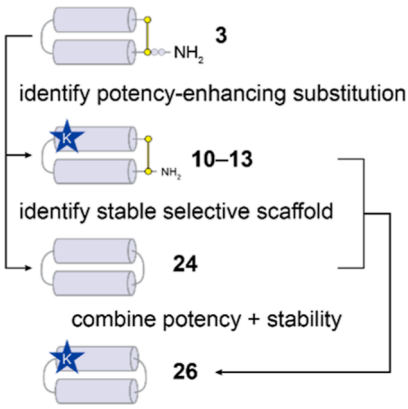

Figure 7. Flow diagram showing the rational improvement of selective antiplasmodial activity and stability for PDIPs.

properties during peptide-based drug development. PDIP analogues are unique in their derivation from a human defense protein, and their selective entry into infected RBCs and membrane-active mechanism of action (lysis of the parasite digestive vacuole) is distinct from that of current antimalarial drugs. These features make the tunable PDIP scaffold a valuable candidate for expanding the range of bioactive molecules available for the development of new antimalarial drugs and combination therapies.

METHODS

Peptide Synthesis and Purification. All peptides were synthesized using automated Fmoc solid phase chemistry (Symphony, Protein Technologies Inc.). Rink amide resin was used to produce peptides with an amidated C-terminus (**3**–**16** and **18**), and 2-chlorotrityl chloride resin was used for peptides with a C-terminal carboxylic acid (**17** and **19**). Linear precursors for backbone cyclic peptides (**20**–**27**) were synthesized on Fmoc-NHNH-chlorotrityl resin prepared as previously described.[64,65] Peptides were deprotected and cleaved from the resin using TFA:H_2O:TIPS (95:2.5:2.5, v/v/v) and collected by precipitating with ice-cold ether. Crude peptides were purified by RP-HPLC using a Shimadzu system and Phenomenex Gemini C18 column with a gradient of solvent B (90% CH_3CN, 0.05% v/v TFA) against solvent A (0.05% TFA v/v).

Disulfide Macrocyclic Peptides. Purified and lyophilized peptides were dissolved at 0.5 mg/mL in 45% CH_3CN and 0.05% TFA (v/v), flushed with nitrogen gas, and oxidized with 20 mol equiv of iodine, as reported before.[30]

Backbone Cyclic Peptides. Linear precursors were synthesized with an N-terminal Cys and C-terminal hydrazide to facilitate cyclization via intramolecular native chemical ligation, as previously described.[33,34] To convert the C-terminal hydrazide to a thioester, purified and lyophilized peptides were dissolved at 3 mM in 6 M GnHCl (pH < 3), with 4-mercaptophenylacetic acid (200 mM) and 9 mM acetyl acetone (3 equiv), and stirred at room temperature for 4 h. Head-to-tail cyclization was achieved by diluting the reaction to achieve a solution of 0.5 mM peptide in 6 M GnHCl, 100 mM NaH_2PO_4, and 50 mM TCEP, with pH adjusted to pH 7, and stirring overnight at room temperature. Disulfide bonds were formed for peptides **20**–**23** by iodine oxidation as described above. Cys residues in precursors for peptides **24**–**27** were desulfurized to Ala by reacting the peptides with 0.25 M TCEP, 3 M GnHCl, 50 mM NaH_2PO_4, 10 mM reduced glutathione, and 50 mM VA-044 (Fujifilm Wako Chemicals), with pH adjusted to 6.5, purged with argon, and incubated overnight at 65 °C.[66] Oxidized or backbone cyclized peptides were purified by RP-HPLC as above. Purity and correct mass of the peptides were simultaneously determined using a Shimadzu LCMS-2020 instrument with a Phenomenex 5 μm C18/300 Å/150 × 2 mm LC column. HPLC traces are shown in Figure S1, with LC peak integration and MS characterization provided for analogues with apparent shoulder peaks or impurities (≤5%) in Figure S2. Observed masses derived from +4 m/z ions are compared to calculated masses, as shown in Table S1.

Overall Structure Determination. CD spectra between 185 and 260 nm were collected for 50 μM peptides in aqueous solution (100 mM NaF, 10 mM KH_2PO_4, pH 7.5) using a Jasco J810 spectropolarimeter, as reported before.[30] CD spectra were also collected in 50% aqueous solution and 50% trifluoroethanol (v/v) for peptides **2** and **15**. MRE was calculated using the formula

$$\text{MRE} = \text{millidegrees}/(\text{molar concentration}) \times (\text{lightpath in mm}) \times (\text{number of residues})$$

The % helicity was determined from the minimal MRE between 218 and 222 nm.[67,68]

Resistance to Breakdown by Serum Proteases. Peptide stability was determined by incubating 5 μM peptide in 25% (v/v) human serum (Sigma-Aldrich) in PBS for 24 h at 37 °C. The amount of peptide remaining after 24 h incubation was calculated relative to 0 h controls by precipitating serum proteins with 2% (v/v) TFA in CH_3CN as before[30] and running the soluble fraction (with recovered peptide) on a Triple TOF 5600 mass spectrometer (AB SCIEX). The $[M + 4]^{4+}$ m/z peak corresponding to full-length peptide mass was identified using SCIEX Analyst software, and the area under the curve was determined using SCIEX MultiQuant software. The average of three 0 h controls was used to determine 100% recovered peptide, and % recovery was determined for three technical repeats of each peptide.

Membrane Binding and Selectivity. Small unilamellar vesicles were prepared by resuspending dried films of synthetic POPC or a 4:1 mixture of POPC and POPS (Avanti Polar Lipids via Sigma-Aldrich) in 10 mM HEPES, 150 mM NaCl (pH 7.4) (SPR running buffer), followed by freeze–thaw cycles and extrusion through a 50 nm membrane.[30] Peptide–lipid interactions were examined by using SPR with an L1 chip (Cytiva) on a Biacore T200 instrument. Lipid vesicles were deposited until a steady-state plateau was reached, when we assume that lipid bilayers have formed.[69] Serial dilutions of peptides from 4 to 32 μM in SPR running buffer were injected over deposited lipid bilayers for 180 s (association). Dissociation was followed for 600 s, while SPR running buffer continued to flow over the chip surface. Response units were converted to P/L using the following equation

$$\text{P/L} = (\text{RU peptide/mw peptide})/(\text{RU lipid/mw lipid})$$

P/L at the end of the association phase (170 s) was used to prepare dose–response curves, which were fitted using One-Site specific binding (GraphPad Prism v10). P/L for 16 μM peptides was used to compare between binding to POPC/POPS (4:1) and POPC.

***In Vitro* Activity Against P. falciparum.** *P. falciparum* 3D7 parasites were cultured in human RBCs (from screened volunteers via Red Cross Lifeblood). Culture medium

https://doi.org/10.1021/acsinfecdis.4c00276
ACS Infect. Dis. 2024, 10, 2899–2912

comprised RPMI1640 (Sigma) supplemented with 2.5 mg/mL Albumax II (Thermo Fisher Scientific), 25 mM HEPES, 0.37 mM hypoxanthine, and 5% human serum (Sigma). Growth inhibition assays were performed in the serum-containing media above or media supplemented with 5 mg/mL Albumax II and no serum, as previously described.[42] In brief, synchronized parasite cultures (sorbitol enrichment of early ring stage) were plated at 2% parasitemia and 0.3% hematocrit in 384-well CellCarrier Ultra poly-D-lysine imaging plates (Revvity), treated with serially diluted peptides in PBS (with final 0.4% v/v DMSO) starting from 67.5 μM, and incubated for 72 h at 37 °C, 5% CO_2, and 5% O_2. Inhibition of *P. falciparum* growth was determined for treated samples compared to vehicle (0.4% DMSO, 0% inhibition) and an in-plate positive control (5 μM puromycin, 100% inhibition) by staining nuclei with 2-(4-amidinophenyl)-1H-indole-6-carboxamidine (DAPI). Stained nuclei were detected using a Phenix confocal imaging system (Revvity) with images analyzed as previously described using Acapella or Harmony spot detection software.[42,43] Dose−response curves were fitted with GraphPad Prism (v10) using [inhibitor] versus response with variable slope and constraining the top to 100% (See Figure S5). IC_{50} values derived from dose−response curves are shown in Table 1. Data represent the mean and standard error from two biological replicates.

Peptide Uptake Studies. Peptides **3**, **14**, and **15** were labeled in the presence of TCEP, using dichloroacetone to form an acetone bridge between Cys residues and oxime ligation using 2 mol equiv AlexaFluor-488 (A488) hydroxylamine (Thermo Fisher Scientific), as previously described.[30] Labeled peptides were purified by RP-HPLC as described above.

Cultures of uninfected and trophozoite-infected human RBCs (approximately 28−36 h post-invasion; 3−5% parasitemia) were incubated with A488-labeled peptides (0.625−40 μM) in culture medium supplemented with 5 mg/mL Albumax II and no serum (as above) for 1 h (our unpublished live-cell uptake studies indicate that this is sufficient time for significant peptide uptake). Treated cells were washed twice with serum-free culture medium to remove any residual unincorporated peptide and then fixed with 1% (w/v) formaldehyde [CytofixTM (BD Biosciences) diluted 1/4 with PBS] for at least 24 h at 4 °C. For the peptide uptake studies, fixed cells were washed with PBS containing 1% (w/v) bovine serum albumin and then stained with 5 mg/mL Hoechst 33342 (Life Technologies) for 5 min at 4 °C. Fluorescence intensity signals were measured by flow cytometry using an LSR Fortessa cell analyzer (BD Biosciences); at least 100,000 events were collected per sample (350 nm laser, 450/50 filter for Hoechst; 488 nm laser, 530/30 filter for A488). Percentages of infected cells (Hoechst-stained nuclei) and mean fluorescence intensity of cells (with the A488-labeled peptide) were identified and enumerated using FlowJo software (BD Biosciences). For the microscopy image shown in Figure 1, *P. falciparum* (trophozoite-stage) cultured human RBCs, either untreated or treated with PDIP-A488 (20 μM for 1 h), were washed and fixed as described for the peptide uptake studies. The fixed cells were then washed and diluted into PBS, smeared onto glass slides coated with polyethylenimine (0.1% v/v), air-dried (5 min), and then washed again in PBS before mounting under coverslips (#1 from Menzel-Glaser) in SlowFade Gold Antifade Mountant with DAPI (Thermo Fisher Scientific). Slides were examined at room temperature using an Axio Observer inverted fluorescence microscope using 630× magnification and coupled to an Axiocam 503 monochrome camera (Zeiss). Images were acquired and processed using a ZEN microscope and imaging software (Zeiss).

Hemolysis of Uninfected RBCs. Blood was collected from a healthy human volunteer directly into PBS. RBCs were pelleted by centrifuging at 1000 g for 1 min; the supernatant was removed, and the cells were washed three times with PBS. RBCs were plated at 0.5% hematocrit in PBS into 96-well plates, and an equal volume of peptides serially diluted in PBS were added to the wells. PBS (0% lysis) and 0.1% (v/v) Triton-X 100 (100% lysis) controls were included. Plates were incubated for 1 h at 37 °C, 5% CO_2; then intact cells were pelleted by centrifuging at 500 g for 5 min. The supernatant was transferred to another plate, and release of hemoglobin from lysed cells was detected by measuring the absorbance at 405 nm. Dose−response curves were fitted with GraphPad Prism (v10) using [inhibitor] vs response with variable slope (Figure S6). Minimum hemolytic concentrations (HC_{10}, 10% of RBCs lysed) were interpolated from dose−response curves and are shown in Table 1. Data represent mean and standard error from two biological replicates. Hemolysis assays were also performed for peptides **3**, **10**, **12**, **24**, and **26** under similar conditions to *in vitro P. falciparum* activity experiments (serum-free culture medium supplemented with 5 mg/mL Albumax II), confirming <10% lysis with up to 72 h incubation.

Human Ethics Approvals. Experiments involving human RBCs and serum were performed in accordance with the following ethics approvals: Griffith University Human Research Ethics Exemption Approval 03/08/11019 (*P. falciparum* culture and activity assays); Australian National University Human Research Ethics Committee, approval number 2018/398 (*P. falciparum* culture and peptide uptake studies); and University of Queensland Human Research Ethics Approval number 2022/HE000300 (RBC hemolysis assays).

■ ASSOCIATED CONTENT

Supporting Information

The Supporting Information is available free of charge at https://pubs.acs.org/doi/10.1021/acsinfecdis.4c00276.

Peptide amino acid sequence and masses of PDIP analogues; HPLC of the analogues; integration of LC trace and MS spectra for analogues with shoulder peaks; sequence homology to the PF4 AMP domain from a nonredundant protein database search; additional structural and cell-penetrating characterization performed for inactive peptide **15** compared to parent peptides **2** and **3**; dose−response curves for *in vitro* activity against *P. falciparum*; dose−response curves for RBC hemolysis; and the relationship between peptide interaction with negatively charged lipid bilayers and *in vitro* antiplasmodial activity (PDF)

■ AUTHOR INFORMATION

Corresponding Authors

Nicole Lawrence − *Institute for Molecular Bioscience and Australian Research Council Centre of Excellence for Innovations in Peptide and Protein Science, The University of Queensland, Brisbane, Queensland 4072, Australia;* orcid.org/0000-0002-9013-1770; Email: n.lawrence@imb.uq.edu.au

Brendan J. McMorran − *The John Curtin School of Medical Research, College of Health and Medicine, Australian National*

https://doi.org/10.1021/acsinfecdis.4c00276
ACS Infect. Dis. 2024, 10, 2899−2912

University, Canberra, Australian Capital Territory 2601, Australia; Email: brendan.mcmorran@anu.edu.au

Authors

Thomas N. G. Handley − *Department of Radiopharmaceutical Sciences, Cancer Imaging, The Peter MacCallum Cancer Centre, Victoria 3000, Australia; Sir Peter MacCallum Department of Oncology, The University of Melbourne, Victoria 3010, Australia*

Simon J. de Veer − *Institute for Molecular Bioscience and Australian Research Council Centre of Excellence for Innovations in Peptide and Protein Science, The University of Queensland, Brisbane, Queensland 4072, Australia;* orcid.org/0000-0002-7041-9937

Maxim D. Harding − *Institute for Molecular Bioscience and Australian Research Council Centre of Excellence for Innovations in Peptide and Protein Science, The University of Queensland, Brisbane, Queensland 4072, Australia*

Alicja Andraszek − *Institute for Molecular Bioscience and Australian Research Council Centre of Excellence for Innovations in Peptide and Protein Science, The University of Queensland, Brisbane, Queensland 4072, Australia*

Lachlan Hall − *Institute for Molecular Bioscience and Australian Research Council Centre of Excellence for Innovations in Peptide and Protein Science, The University of Queensland, Brisbane, Queensland 4072, Australia;* orcid.org/0009-0001-8177-0247

Karoline D. Raven − *The John Curtin School of Medical Research, College of Health and Medicine, Australian National University, Canberra, Australian Capital Territory 2601, Australia;* orcid.org/0000-0002-7579-9721

Sandra Duffy − *Discovery Biology, Centre for Cellular Phenomics, School of Environment and Science, Griffith University, Nathan, Queensland 4111, Australia*

Vicky M. Avery − *Discovery Biology, Centre for Cellular Phenomics, School of Environment and Science, Griffith University, Nathan, Queensland 4111, Australia*

David J. Craik − *Institute for Molecular Bioscience and Australian Research Council Centre of Excellence for Innovations in Peptide and Protein Science, The University of Queensland, Brisbane, Queensland 4072, Australia;* orcid.org/0000-0003-0007-6796

Lara R. Malins − *Research School of Chemistry and Australian Research Council Centre of Excellence for Innovations in Peptide and Protein Science, Australian National University, Canberra, Australian Capital Territory 2601, Australia;* orcid.org/0000-0002-7691-6432

Complete contact information is available at: https://pubs.acs.org/10.1021/acsinfecdis.4c00276

Notes

The authors declare no competing financial interest.

■ ACKNOWLEDGMENTS

This work was supported by funding from the Australian National Health and Medical Research Council (1183927 to B. J. M., N. L., and L. R. M.), US Department of Defense grant (PR210354 to D. J. C. and N. L.), and the Australian Research Council Centre of Excellence for Innovations in Peptide and Protein Science (CE200100012). D.J.C. was supported by NHMRC grant (2009564). S.D. was supported by a Griffith University Postdoctoral Fellowship (GUPF_23_24). The authors would like to thank Yen-Hua Huang, Bhavesh Khatri, and Lai Yue Chan for peptide synthesis; and Megan Drew, Huma Sohail, and Kiran Javed for malaria parasite culture and support in performing preliminary activity assays that guided analogue design.

■ REFERENCES

(1) World Health Organisation. *World Malaria Report 2023; Licence: CC BY-NC-SA 3.0 IGO*: Geneva, 2023.

(2) Siqueira-Neto, J. L.; Wicht, K. J.; Chibale, K.; Burrows, J. N.; Fidock, D. A.; Winzeler, E. A. Antimalarial drug discovery: progress and approaches. *Nat. Rev. Drug Discovery* **2023**, *22* (10), 807−826.

(3) Plowe, C. V. Malaria chemoprevention and drug resistance: a review of the literature and policy implications. *Malar. J.* **2022**, *21* (1), 104.

(4) Balikagala, B.; Fukuda, N.; Ikeda, M.; Katuro, O. T.; Tachibana, S.-I.; Yamauchi, M.; Opio, W.; Emoto, S.; Anywar, D. A.; Kimura, E.; Palacpac, N. M. Q.; Odongo-Aginya, E. I.; Ogwang, M.; Horii, T.; Mita, T. Evidence of artemisinin-resistant malaria in Africa. *N. Engl. J. Med.* **2021**, *385* (13), 1163−1171.

(5) Jeang, B.; Zhong, D.; Lee, M. C.; Atieli, H.; Yewhalaw, D.; Yan, G. Molecular surveillance of Kelch 13 polymorphisms in *Plasmodium falciparum* isolates from Kenya and Ethiopia. *Malar. J.* **2024**, *23* (1), 36.

(6) Conrad, M. D.; Rosenthal, P. J. Antimalarial drug resistance in Africa: the calm before the storm? *Lancet Infect. Dis.* **2019**, *19* (10), e338−e351.

(7) Schäfer, T. M.; Pessanha de Carvalho, L.; Inoue, J.; Kreidenweiss, A.; Held, J. The problem of antimalarial resistance and its implications for drug discovery. *Expert Opin. Drug Discovery* **2024**, *19* (2), 209−224.

(8) Ippolito, M. M.; Moser, K. A.; Kabuya, J. B.; Cunningham, C.; Juliano, J. J. Antimalarial drug resistance and implications for the WHO global technical strategy. *Curr. Epidemiol. Rep.* **2021**, *8* (2), 46−62.

(9) Boni, M. F. Breaking the cycle of malaria treatment failure. *Front. Epidemiol.* **2022**, *2*, 1041896.

(10) Chico, R. M.; Pittrof, R.; Greenwood, B.; Chandramohan, D. Azithromycin-chloroquine and the intermittent preventive treatment of malaria in pregnancy. *Malar. J.* **2008**, *7* (1), 255.

(11) Gaillard, T.; Boxberger, M.; Madamet, M.; Pradines, B. Has doxycycline, in combination with anti-malarial drugs, a role to play in intermittent preventive treatment of *Plasmodium falciparum* malaria infection in pregnant women in Africa? *Malar. J.* **2018**, *17* (1), 469.

(12) Qiu, D.; Pei, J. V.; Rosling, J. E. O.; Thathy, V.; Li, D.; Xue, Y.; Tanner, J. D.; Penington, J. S.; Aw, Y. T. V.; Aw, J. Y. H.; Xu, G.; Tripathi, A. K.; Gnadig, N. F.; Yeo, T.; Fairhurst, K. J.; Stokes, B. H.; Murithi, J. M.; Kümpornsin, K.; Hasemer, H.; Dennis, A. S. M.; Ridgway, M. C.; Schmitt, E. K.; Straimer, J.; Papenfuss, A. T.; Lee, M. C. S.; Corry, B.; Sinnis, P.; Fidock, D. A.; van Dooren, G. G.; Kirk, K.; Lehane, A. M. A G358S mutation in the *Plasmodium falciparum* Na+ pump PfATP4 confers clinically-relevant resistance to cipargamin. *Nat. Commun.* **2022**, *13* (1), 5746.

(13) Schmitt, E. K.; Ndayisaba, G.; Yeka, A.; Asante, K. P.; Grobusch, M. P.; Karita, E.; Mugerwa, H.; Asiimwe, S.; Oduro, A.; Fofana, B.; Doumbia, S.; Su, G.; Csermak Renner, K.; Venishetty, V. K.; Sayyed, S.; Straimer, J.; Demin, I.; Barsainya, S.; Boulton, C.; Gandhi, P. Efficacy of cipargamin (KAE609) in a randomized, phase II dose-escalation study in adults in Sub-Saharan Africa with uncomplicated *Plasmodium falciparum* malaria. *Clin. Infect. Dis.* **2022**, *74* (10), 1831−1839.

(14) Zasloff, M. Antimicrobial peptides of multicellular organisms. *Nature* **2002**, *415* (6870), 389−395.

(15) Hancock, R. E. W.; Diamond, G. The role of cationic antimicrobial peptides in innate host defences. *Trends Microbiol.* **2000**, *8* (9), 402−410.

(16) Hancock, R. E. W.; Sahl, H.-G. Antimicrobial and host-defense peptides as new anti-infective therapeutic strategies. *Nat. Biotechnol.* **2006**, *24* (12), 1551−1557.

(17) Fadok, V. A.; Voelker, D. R.; Campbell, P. A.; Cohen, J. J.; Bratton, D. L.; Henson, P. M. Exposure of phosphatidylserine on the surface of apoptotic lymphocytes triggers specific recognition and removal by macrophages. *J. Immunol.* **1992**, *148* (7), 2207−2216.

(18) Sharma, B.; Kanwar, S. S. Phosphatidylserine: A cancer cell targeting biomarker. *Semin. Cancer Biol.* **2018**, *52*, 17−25.
(19) Engelbrecht, D.; Coetzer, T. L. *Plasmodium falciparum* exhibits markers of regulated cell death at high population density *in vitro*. *Parasitol. Int.* **2016**, *65* (6), 715−727.
(20) Fraser, M.; Jing, W.; Bröer, S.; Kurth, F.; Sander, L.-E.; Matuschewski, K.; Maier, A. G. Breakdown in membrane asymmetry regulation leads to monocyte recognition of *P. falciparum*-infected red blood cells. *PLoS Pathog.* **2021**, *17* (2), No. e1009259.
(21) Zorzi, A.; Deyle, K.; Heinis, C. Cyclic peptide therapeutics: past, present and future. *Curr. Opin. Chem. Biol.* **2017**, *38*, 24−29.
(22) Peschel, A.; Sahl, H.-G. The co-evolution of host cationic antimicrobial peptides and microbial resistance. *Nat. Rev. Microbiol.* **2006**, *4* (7), 529−536.
(23) Xuan, J.; Feng, W.; Wang, J.; Wang, R.; Zhang, B.; Bo, L.; Chen, Z.-S.; Yang, H.; Sun, L. Antimicrobial peptides for combating drug-resistant bacterial infections. *Drug Resist. Updat.* **2023**, *68*, 100954.
(24) Le, C. F.; Fang, C. M.; Sekaran, S. D. Intracellular targeting mechanisms by antimicrobial peptides. *Antimicrob. Agents Chemother.* **2017**, *61* (4), No. e02340.
(25) Brogden, K. A. Antimicrobial peptides: pore formers or metabolic inhibitors in bacteria? *Nat. Rev. Microbiol.* **2005**, *3* (3), 238−250.
(26) Amiss, A. S.; Henriques, S. T.; Lawrence, N. Antimicrobial peptides provide wider coverage for targeting drug-resistant bacterial pathogens. *Pept. Sci.* **2022**, *114* (2), No. e24246.
(27) McMorran, B. J.; Wieczorski, L.; Drysdale, K. E.; Chan, J. A.; Huang, H. M.; Smith, C.; Mitiku, C.; Beeson, J. G.; Burgio, G.; Foote, S. J. Platelet factor 4 and Duffy antigen required for platelet killing of *Plasmodium falciparum*. *Science* **2012**, *338* (6112), 1348−1351.
(28) Love, M. S.; Millholland, M. G.; Mishra, S.; Kulkarni, S.; Freeman, K. B.; Pan, W.; Kavash, R. W.; Costanzo, M. J.; Jo, H.; Daly, T. M.; Williams, D. R.; Kowalska, M. A.; Bergman, L. W.; Poncz, M.; DeGrado, W. F.; Sinnis, P.; Scott, R. W.; Greenbaum, D. C. Platelet factor 4 activity against *P. falciparum* and its translation to nonpeptidic mimics as antimalarials. *Cell Host Microbe* **2012**, *12* (6), 815−823.
(29) Yeaman, M. R.; Yount, N. Y.; Waring, A. J.; Gank, K. D.; Kupferwasser, D.; Wiese, R.; Bayer, A. S.; Welch, W. H. Modular determinants of antimicrobial activity in platelet factor-4 family kinocidins. *Biochim. Biophys. Acta* **2007**, *1768* (3), 609−619.
(30) Lawrence, N.; Dennis, A. S. M.; Lehane, A. M.; Ehmann, A.; Harvey, P. J.; Benfield, A. H.; Cheneval, O.; Henriques, S. T.; Craik, D. J.; McMorran, B. J. Defense peptides engineered from human platelet factor 4 kill *Plasmodium* by selective membrane disruption. *Cell Chem. Biol.* **2018**, *25* (9), 1140−1150.e5.
(31) Tawk, L.; Chicanne, G.; Dubremetz, J. F.; Richard, V.; Payrastre, B.; Vial, H. J.; Roy, C.; Wengelnik, K. Phosphatidylinositol 3-phosphate, an essential lipid in *Plasmodium*, localizes to the food vacuole membrane and the apicoplast. *Eukaryot. Cell* **2010**, *9* (10), 1519−1530.
(32) Clarke, R. J.; Hossain, K. R.; Cao, K. Physiological roles of transverse lipid asymmetry of animal membranes. *BBA. Biomembranes* **2020**, *1862* (10), 183382.
(33) Dawson, P. E.; Muir, T. W.; Clark-Lewis, I.; Kent, S. B. H. Synthesis of proteins by native chemical ligation. *Science* **1994**, *266* (5186), 776−779.
(34) Cistrone, P. A.; Bird, M. J.; Flood, D. T.; Silvestri, A. P.; Hintzen, J. C. J.; Thompson, D. A.; Dawson, P. E. Native chemical ligation of peptides and proteins. *Curr. Protoc. Chem. Biol.* **2019**, *11* (1), No. e61.
(35) Lawrence, N.; Philippe, G. J. B.; Harvey, P. J.; Condon, N. D.; Benfield, A. H.; Cheneval, O.; Craik, D. J.; Troeira Henriques, S. Cyclic peptide scaffold with ability to stabilize and deliver a helical cell-impermeable cargo across membranes of cultured cancer cells. *RSC Chem. Biol.* **2020**, *1* (5), 405−420.
(36) Palombi, I. R.; Lawrence, N.; White, A. M.; Gare, C. L.; Craik, D. J.; McMorran, B. J.; Malins, L. R. Development of antiplasmodial peptide-drug conjugates using a human protein-derived cell-penetrating peptide with selectivity for infected cells. *Bioconjugate Chem.* **2023**, *34* (6), 1105−1113.
(37) Assem, N.; Ferreira, D. J.; Wolan, D. W.; Dawson, P. E. Acetone-linked peptides: a convergent approach for peptide macrocyclization and labeling. *Angew. Chem., Int. Ed. Engl.* **2015**, *54* (30), 8665−8668.
(38) Johnson, M.; Zaretskaya, I.; Raytselis, Y.; Merezhuk, Y.; McGinnis, S.; Madden, T. L. NCBI BLAST: a better web interface. *Nucleic Acids Res.* **2008**, *36* (Web Server), W5−W9.
(39) Torcato, I. M.; Huang, Y. H.; Franquelim, H. G.; Gaspar, D. D.; Craik, D. J.; Castanho, M. A.; Henriques, S. T. The antimicrobial activity of Sub3 is dependent on membrane binding and cell-penetrating ability. *Chembiochem* **2013**, *14* (15), 2013−2022.
(40) Henriques, S. T.; Lawrence, N.; Chaousis, S.; Ravipati, A. S.; Cheneval, O.; Benfield, A. H.; Elliott, A. G.; Kavanagh, A. M.; Cooper, M. A.; Chan, L. Y.; Huang, Y. H.; Craik, D. J. Redesigned spider peptide with improved antimicrobial and anticancer properties. *ACS Chem. Biol.* **2017**, *12* (9), 2324−2334.
(41) Wiedman, G.; Kim, S. Y.; Zapata-Mercado, E.; Wimley, W. C.; Hristova, K. pH-triggered, macromolecule-sized poration of lipid bilayers by synthetically evolved peptides. *J. Am. Chem. Soc.* **2017**, *139* (2), 937−945.
(42) Duffy, S.; Avery, V. M. Development and optimization of a novel 384-well anti-malarial imaging assay validated for high-throughput screening. *Am. J. Trop. Med. Hyg.* **2012**, *86* (1), 84−92.
(43) Guiguemde, W. A.; Shelat, A. A.; Bouck, D.; Duffy, S.; Crowther, G. J.; Davis, P. H.; Smithson, D. C.; Connelly, M.; Clark, J.; Zhu, F.; Jiménez-Díaz, M. B.; Martinez, M. S.; Wilson, E. B.; Tripathi, A. K.; Gut, J.; Sharlow, E. R.; Bathurst, I.; Mazouni, F. E.; Fowble, J. W.; Forquer, I.; McGinley, P. L.; Castro, S.; Angulo-Barturen, I.; Ferrer, S.; Rosenthal, P. J.; Derisi, J. L.; Sullivan, D. J.; Lazo, J. S.; Roos, D. S.; Riscoe, M. K.; Phillips, M. A.; Rathod, P. K.; Van Voorhis, W. C.; Avery, V. M.; Guy, R. K. Chemical genetics of *Plasmodium falciparum*. *Nature* **2010**, *465* (7296), 311−315.
(44) Castro, J.; Grundy, L.; Deiteren, A.; Harrington, A. M.; O'Donnell, T.; Maddern, J.; Moore, J.; Garcia-Caraballo, S.; Rychkov, G. Y.; Yu, R.; Kaas, Q.; Craik, D. J.; Adams, D. J.; Brierley, S. M. Cyclic analogues of α-conotoxin Vc1.1 inhibit colonic nociceptors and provide analgesia in a mouse model of chronic abdominal pain. *Br. J. Pharmacol.* **2018**, *175* (12), 2384−2398.
(45) Vernen, F.; Harvey, P. J.; Dias, S. A.; Veiga, A. S.; Huang, Y.-H.; Craik, D. J.; Lawrence, N.; Troeira Henriques, S. Characterization of tachyplesin peptides and their cyclized analogues to improve antimicrobial and anticancer properties. *Int. J. Mol. Sci.* **2019**, *20* (17), 4184.
(46) Saska, I.; Gillon, A. D.; Hatsugai, N.; Dietzgen, R. G.; Hara-Nishimura, I.; Anderson, M. A.; Craik, D. J. An asparaginyl endopeptidase mediates *in vivo* protein backbone cyclization. *J. Biol. Chem.* **2007**, *282* (40), 29721−29728.
(47) Jackson, M. A.; Gilding, E. K.; Shafee, T.; Harris, K. S.; Kaas, Q.; Poon, S.; Yap, K.; Jia, H.; Guarino, R.; Chan, L. Y.; Durek, T.; Anderson, M. A.; Craik, D. J. Molecular basis for the production of cyclic peptides by plant asparaginyl endopeptidases. *Nat. Commun.* **2018**, *9* (1), 2411.
(48) Jia, F.; Wang, J.; Peng, J.; Zhao, P.; Kong, Z.; Wang, K.; Yan, W.; Wang, R. D-amino acid substitution enhances the stability of antimicrobial peptide polybia-CP. *Acta Biochim. Biophys. Sin.* **2017**, *49* (10), 916−925.
(49) Böttger, R.; Hoffmann, R.; Knappe, D. Differential stability of therapeutic peptides with different proteolytic cleavage sites in blood, plasma and serum. *PLoS One* **2017**, *12* (6), No. e0178943.
(50) Lu, J.; Xu, H.; Xia, J.; Ma, J.; Xu, J.; Li, Y.; Feng, J. D- and unnatural amino acid substituted antimicrobial peptides with improved proteolytic resistance and their proteolytic degradation characteristics. *Front. Microbiol.* **2020**, *11*, 563030.
(51) Ayogu, E. E.; Mosanya, A. U.; Onuh, J. C.; Adibe, M. O.; Ubaka, C. M.; Ukwe, C. V. Direct medical cost of treatment of uncomplicated malaria after the adoption of artemisinin-based combination therapy in Nigeria. *J. Appl. Pharm. Sci.* **2021**, *11* (9), 029−034.
(52) Ismail, N. E.; Jimam, N. S.; Goh, K. W.; Tan, C. S.; Ming, L. C. Economic burdens of uncomplicated malaria in primary health care (PHC) facilities of Plateau State, Nigeria: patients' perspectives. *Int. J. Environ. Res. Public Health* **2023**, *20* (2), 1093.

https://doi.org/10.1021/acsinfecdis.4c00276
ACS Infect. Dis. 2024, 10, 2899−2912

(53) Wani, K. I.; Choudhary, S.; Zehra, A.; Naeem, M.; Weathers, P.; Aftab, T. Enhancing artemisinin content in and delivery from Artemisia annua: a review of alternative, classical, and transgenic approaches. *Planta* **2021**, *254* (2), 29.
(54) Kayani, W. K.; Kiani, B. H.; Dilshad, E.; Mirza, B. Biotechnological approaches for artemisinin production in Artemisia. *World J. Microbiol. Biotechnol.* **2018**, *34* (4), 54.
(55) Medicines for Malaria Venture. *African Drug Manufacturing*. 2024. https://www.mmv.org/our-work/access-to-medicines/african-drug-manufacturing (accessed May 31, 2024).
(56) Wang, J.; Chen, L.; Qin, S.; Xie, M.; Luo, S.-Z.; Li, W. Advances in biosynthesis of peptide drugs: Technology and industrialization. *Biotechnol. J.* **2024**, *19* (1), 2300256.
(57) Yap, K.; Du, J.; Looi, F. Y.; Tang, S. R.; de Veer, S. J.; Bony, A. R.; Rehm, F. B. H.; Xie, J.; Chan, L. Y.; Wang, C. K.; Adams, D. J.; Lua, L. H. L.; Durek, T.; Craik, D. J. An environmentally sustainable biomimetic production of cyclic disulfide-rich peptides. *Green Chem.* **2020**, *22* (15), 5002−5016.
(58) Hoelscher, M. P.; Forner, J.; Calderone, S.; Krämer, C.; Taylor, Z.; Loiacono, F. V.; Agrawal, S.; Karcher, D.; Moratti, F.; Kroop, X.; Bock, R. Expression strategies for the efficient synthesis of antimicrobial peptides in plastids. *Nat. Commun.* **2022**, *13* (1), 5856.
(59) Jackson, M. A.; Xie, J.; Nguyen, L. T. T.; Wang, X.; Yap, K.; Harvey, P. J.; Gilding, E. K.; Craik, D. J. Plant-based production of an orally active cyclotide for the treatment of multiple sclerosis. *Transgenic Res.* **2023**, *32* (1−2), 121−133.
(60) Jackson, M. A.; Yap, K.; Poth, A. G.; Gilding, E. K.; Swedberg, J. E.; Poon, S.; Qu, H.; Durek, T.; Harris, K.; Anderson, M. A.; Craik, D. J. Rapid and scalable plant-based production of a potent plasmin inhibitor peptide. *Front. Plant Sci.* **2019**, *10*, No. 602.
(61) Munro, B. A.; McMorran, B. J. Antimalarial drug strategies to target *Plasmodium* x2gametocytes. *Parasitologia* **2022**, *2* (2), 101−124.
(62) Andersson, D. I.; Hughes, D.; Kubicek-Sutherland, J. Z. Mechanisms and consequences of bacterial resistance to antimicrobial peptides. *Drug Resist. Updat.* **2016**, *26*, 43−57.
(63) Benfield, A. H.; Vernen, F.; Young, R. S. E.; Nadal-Bufí, F.; Hammerlindl, H.; Craik, D. J.; Schaider, H.; Lawrence, N.; Blanksby, S. J.; Henriques, S. T. Cyclic tachyplesin I kills proliferative, non-proliferative and drug-resistant melanoma cells without inducing resistance. *Pharmacol. Res.* **2024**, *207*, No. 107298.
(64) Huang, Y.-C.; Chen, C.-C.; Li, S.-J.; Gao, S.; Shi, J.; Li, Y.-M. Facile synthesis of C-terminal peptide hydrazide and thioester of NY-ESO-1 (A39-A68) from an Fmoc-hydrazine 2-chlorotrityl chloride resin. *Tetrahedron* **2014**, *70* (18), 2951−2955.
(65) Bird, M. J.; Dawson, P. E. A shelf stable Fmoc hydrazine resin for the synthesis of peptide hydrazides. *Pept. Sci.* **2022**, *114* (5), No. e24268.
(66) Cergol, K. M.; Thompson, R. E.; Malins, L. R.; Turner, P.; Payne, R. J. One-pot peptide ligation-desulfurization at glutamate. *Org. Lett.* **2014**, *16* (1), 290−293.
(67) Greenfield, N. J. Using circular dichroism spectra to estimate protein secondary structure. *Nat. Protoc.* **2006**, *1* (6), 2876−2890.
(68) Shepherd, N. E.; Hoang, H. N.; Abbenante, G.; Fairlie, D. P. Single turn peptide alpha helices with exceptional stability in water. *J. Am. Chem. Soc.* **2005**, *127* (9), 2974−2983.
(69) Figueira, T. N.; Freire, J. M.; Cunha-Santos, C.; Heras, M.; Gonçalves, J.; Moscona, A.; Porotto, M.; Salomé Veiga, A.; Castanho, M. A. R. B. Quantitative analysis of molecular partition towards lipid membranes using surface plasmon resonance. *Sci. Rep.* **2017**, *7* (1), 45647.

https://doi.org/10.1021/acsinfecdis.4c00276
ACS Infect. Dis. 2024, 10, 2899−2912